J Appl Biomed
DOI: 10.32725/jab.2023.021
journal homepage: http://jab.zsf.jcu.cz

Journal of Applied Biomedicine

Original research article

Naringin inhibits P2X4 receptor expression on satellite glial cells in the neonatal rat dorsal root ganglion

Hongji Wang [1], Lisha Chen [1], Juping Xing [1], Xiangchao Shi [1], Changshui Xu [1, 2, 3, 4] *

[1] *Basic Medical College of Nanchang University, Department of Physiology, Nanchang, 330006, P.R. China*
[2] *Jiangxi Provincial Key Laboratory of autonomic nervous function and disease, Nanchang, 330006, P.R. China*
[3] *Jiangxi Medical College, School of Clinical Medicine, Shangrao, 334000, P.R. China*
[4] *Jiangxi Medical College, The First Affiliated Hospital, Shangrao, 334000, P.R. China*

Abstract
Naringin inhibits inflammation and oxidative stress, the P2 purinoreceptor X4 receptor (P2X4R) is associated with glial cell activation and inflammation, the purpose of this study is to investigate the effects of naringin on P2X4 receptor expression on satellite glial cells (SGCs) and its possible mechanisms. ATP promoted the SGC activation and upregulated P2X4R expression; naringin inhibited SGC activation, decreased expression of P2X4R, P38 MAPK/ERK, and NF-κB, and reduced levels of Ca^{2+}, TNF-α, and IL-1β in SGCs in an ATP-containing environment. These findings suggest that naringin attenuates the ATP-induced SGC activation and reduces P2X4R expression via the Ca^{2+}-P38 MAPK/ERK-NF-κB pathway.

Keywords: Glial cell activation; Inflammation; Naringin; P2X4R; Satellite glial cells

Highlights:
- P2X4R is involved in ATP-induced SGC activation.
- Naringin inhibits ATP-induced SGC activation involving P2X4R.
- The MAPK signaling pathway is involved in the inhibitory effect of naringin on P2X4R expression.

Abbreviations:
DRG, Dorsal root ganglion; GFAP, Glial fibrillary acidic protein; HGHF, High glucose and high free-fat; IL-1β, Interleukin-1 beta; LPS, Lipopolysaccharide; MAPK, Mitogen-activated protein kinase; NF-κB, Nuclear factor kappa-B; P2X4R, The P2 purinoreceptor X4 receptor; PBS, Phosphate-buffered saline; SGC, Satellite glial cell; TNF-α, Tumor necrosis factor-alpha

Introduction

Naringin is a natural flavonoid (Bhari et al., 2014; Eom et al., 2021; Hassan et al., 2021) that inhibits glial cell activation and suppresses cellular inflammation by reducing the expression of interleukin (IL)-1β, tumor necrosis factor (TNF)-α, and IL-6 (Li et al., 2022). The P2 purinoreceptor X4 receptor (P2X4R) induces several cell responses upon extracellular ATP stimulation, including intracellular and extracellular ion exchange and cytokine release (Duveau et al., 2020; Suurväli et al., 2017). P2X4R regulates signaling pathways associated with inflammation, and its roles in inflammation and pain have been studied extensively (Kohno and Tsuda, 2021; Montilla et al., 2020). Astragalin and artemisinin inhibit SGC activation by reducing P2X4R expression in SGCs, thereby reducing neuropathic pain (Wang et al., 2020; Ying et al., 2017). P2X4R inhibition also reduces the release of TNF-α and IL-6 through the nucleotide-binding oligomerization domain-like receptor thermal protein domain-associated protein 3 signaling pathway, reducing microglia apoptosis and inflammatory responses (He et al., 2022). Treatment with P2X4R antisense oligonucleotide reduced the release of inflammatory factors, improving rheumatoid arthritis (Li et al., 2014).

Increased TNF-α and IL-1β in glial cells are markers of glial cell activation; when SGCs are stimulated, inflammatory cytokine release increases (Hanani, 2022; Huang et al., 2013; Lee and Kim, 2020; Wang and Xu, 2022), and P2X4R mediates the expression and release of these inflammatory factors (Duveau et al., 2020; Suurväli et al., 2017), suggesting that P2X4R is associated with SGCs activation. In contrast, naringin has anti-inflammatory effects and reduces the release and expression of inflammatory factors. We explored how naringin attenuates ATP-induced SGC activation and expression of P2X4R.

* **Corresponding author:** Changshui Xu, Basic Medical College of Nanchang University, Department of Physiology, Nanchang, 330006, P.R. China; e-mail: changshui-xu@163.com
http://doi.org/10.32725/jab.2023.021
Submitted: 2023-03-04 • Accepted: 2023-11-27 • Prepublished online: 2023-12-04
J Appl Biomed 21/4: 193–199 • EISSN 1214-0287 • ISSN 1214-021X

Materials and methods

Primary culture

Newborn Sprague Dawley rats (Medical Animal Experimental Center of Nanchang University. P. R. China) were euthanized within three days of birth, and the spinal column was cut open to remove the spinal cord. The Ethics Committee of Nanchang University approved the study, and animals were treated according to its Guidelines for the Care and Use of Animals. The dorsal root ganglion (DRG) was removed with pointed forceps and placed in a pre-chilled DMEM/F12 medium (Shanghai Viva Cell Biosciences Ltd., P. R. China). The nerve fibers were carefully stripped from the DRG with scissors and forceps. The DRGs were centrifuged at 5,000 × g for 10 min at 25 °C, the supernatants were discarded, and 0.25% trypsin-EDTA was added and placed in a cell culture incubator for 20 min. DMEM/F12 medium containing 10% fetal bovine serum was added to stop the digestion, then centrifuged at 5,000 × g for 10 min at 25 °C, and the supernatants were discarded. We used 2 ml of medium to resuspend the cells. The suspension was filtered through a cell sieve, and the filtrate was added to a cell culture dish.

The experiment was divided into control, control + naringin, ATP, ATP + naringin, and ATP + dimethyl sulfoxide (DMSO) groups. The final concentration of naringin (Aladdin, CAS.10236-47-2) was 80 μM (Chen et al., 2017). The final concentration of ATP (Solarbio, CAS.987-65-5) was 0.1 mM, and phosphate-buffered saline (PBS) was used as the solvent (Du et al., 2022). When the cell confluence reached about 80%, naringin was added for 12 h, and ATP was added for 3 h for subsequent experiments.

Western blot analysis

RIPA cell lysis solution (Biochem; Cat.no.BKM-RA-Q100) was added to the cells and placed in an ice bath for 20 min. The lysed cells were scraped off and centrifuged at 12,000 × g for 10 min at 4 °C. The supernatants were removed, supplemented with protein loading buffer, incubated in a bath of boiling water for 5 min, and stored at –20 °C. The protein samples were separated by sodium dodecyl sulfate-polyacrylamide electrophoresis and transferred to polyvinylidene fluoride membranes by electroblotting (300 mA, 90 min). The membrane strips were placed in 5% bovine serum albumin for 1.5 h. After washing with Tris-buffered saline-Tween, the strips were incubated overnight at 4 °C with the following primary antibodies: rabbit anti-P2X4 (Alomone Labs; Cat. no. APR-002; 1 : 1000), rabbit anti-p38 (Cell Signaling Technology; Cat. no. D13E1; 1 : 1000), rabbit anti-P-p38 (Cell Signaling Technology; Cat. no. D3F9; 1 : 1000), rabbit anti-p65 (Cell Signaling Technology; Cat. no. D14E12; 1 : 1000), rabbit anti-P-p65 (Cell Signaling Technology; Cat. no. S536; 1 : 1000), rabbit anti-ERK (Cell Signaling Technology; Cat. no. 4695S; 1 : 1000), rabbit anti-P-ERK (Cell Signaling Technology; Cat. no. 4370S; 1 : 1000) or mouse anti-β-actin (OriGene Technologies; Cat no. 18AV0408). The following day, after washing with Tris-buffered saline-Tween, the strips were incubated for 2 h at room temperature with goat anti-mouse IgG (Boster Biological Technology; Cat. no. BST17A13B17B50; 1 : 2000) or goat anti-rabbit IgG (OriGene Technologies; Cat. no. ZB-2301; 1 : 2000). All antibodies were diluted with 5% skimmed milk powder. The chemiluminescence signal was developed using an ECL kit (Fdbio science; Cat. no. FD8020), the signal was measured using autoradiography film, and the protein band densities were analyzed using Image J software (https://imagej.net).

Enzyme-linked immunosorbent assay (ELISA)

According to the tumor necrosis factor-alpha/interleukin-1 beta (TNF-α/IL-1β) ELISA Kit instructions (Wuhan Shenke Experimental Technology Co., Ltd.; Cat. no. 202203-180/Cat. no. 202203-047), standard, blank, and sample wells were set up. Cell culture supernatants were diluted five-fold with sample diluent and loaded into the sample wells, then 50 μl aliquots of the gradient-diluted standard sample were loaded into the standard wells, and finally, 50 μl of sample diluent was loaded into the blank wells. The wells were sealed and placed in a 37 °C water bath for 30 min. After incubation, each well was washed five times with washing solution, and the wells' liquid was patted dry. Then, 50 μl horseradish peroxidase solution was added to the sample and the standard wells and incubated at 37 °C for 30 min. After incubation, each well was washed five times with a washing solution and patted dry. Each well was incubated in the dark room for 15 min with 50 μl of chromogenic reagent, and the reaction was finally stopped by adding 50 μl of termination solution. The absorbance at 450 nm was measured on a microplate reader (PerkinElmer, Inc.).

Immunofluorescence

Slides with cells were washed with PBS and incubated with 4% paraformaldehyde for 20 min. After incubation, slides were washed with PBS and incubated with 0.3% Triton X-100 for 10 min. After washing with PBS, 10% of donkey serum was added, and slides were placed in a light-proof box in a 37 °C water bath for 1 h. Than the cell slides were incubated overnight at 4 °C with rabbit anti-P2X4 (Alomone Labs; Cat. no. APR-002; 1 : 100) or mouse anti-glial fibrillary acidic protein (GFAP) (BioLegend; Cat. no. 644702; 1 : 100). The following day, the cell slides were washed with PBS. Diluted donkey anti-rabbit (Abcam; Cat. no. ab7080; 1:200) or donkey anti-mouse (Abcam; Cat. no. ab98794; 1 : 200) antibodies were added in the cell slides and placed in a 37 °C water bath for 1.5 h. After washing with PBS, an anti-fluorescence quencher (Boster Biological Technology Co., Ltd.) was added, and fluorescence was observed under a confocal microscope (Olympus, Tokyo, Japan). Image J software was used for fluorescence intensity analysis.

Intracellular calcium ion measurement

BBcellProbe F03 solution (Bestbio, Nanjing, China) was diluted 1000 times with DMEM/F12 medium. Cells were washed with PBS. Then 200 μl of diluted working solution was added and incubated for 25 min in a cell culture incubator. After incubation, the cells were washed with PBS, and 200 μl of PBS was added prior to incubation for 15 min at 37 °C. Finally, the probe fluorescence (excitation wavelength 488–495 nm, emission wavelength 516 nm) was measured using a microplate reader.

Statistical analysis

Data were expressed as the mean ± standard deviation, and n represents the number of experiments. Data were analyzed using IBM SPSS Statistics (v. 21.0; IBM Corp., Armonk, NY, USA). Histograms were drawn using GraphPad Prism v. 5.0 (GraphPad Software Inc., San Diego, CA, USA). Analysis of variance was used to assess any significance of differences between groups.

Results

Naringin downregulates P2X4R in SGCs and inhibits ATP-induced SGC activation

P2X4R expression in SGCs was measured using western blotting, and P2X4R expression (Fig. 1a) was significantly increased under the stimulation of ATP ($P < 0.001$), while naringin inhibited P2X4R upregulation ($P < 0.01$).

GFAP is one of markers of SGC activation. GFAP expression in SGCs was measured to evaluate SGC activation using cellular immunofluorescence (Fig. 1b). GFAP expression was significantly increased under the stimulation of ATP ($P < 0.001$), while naringin inhibited GFAP expression ($P < 0.001$; Fig. 1c), suggesting that naringin inhibits SGC activation. P2X4R and GFAP coexpression was measured using cellular immunofluorescence (Fig. 1b); ATP significantly increased P2X4R and GFAP coexpression (Fig. 1d) ($P < 0.001$), and the fluorescence intensity of P2X4R and GAFP coexpression decreased with the addition of naringin ($P < 0.001$). These findings suggest that naringin inhibits SGC activation and P2X4R expression.

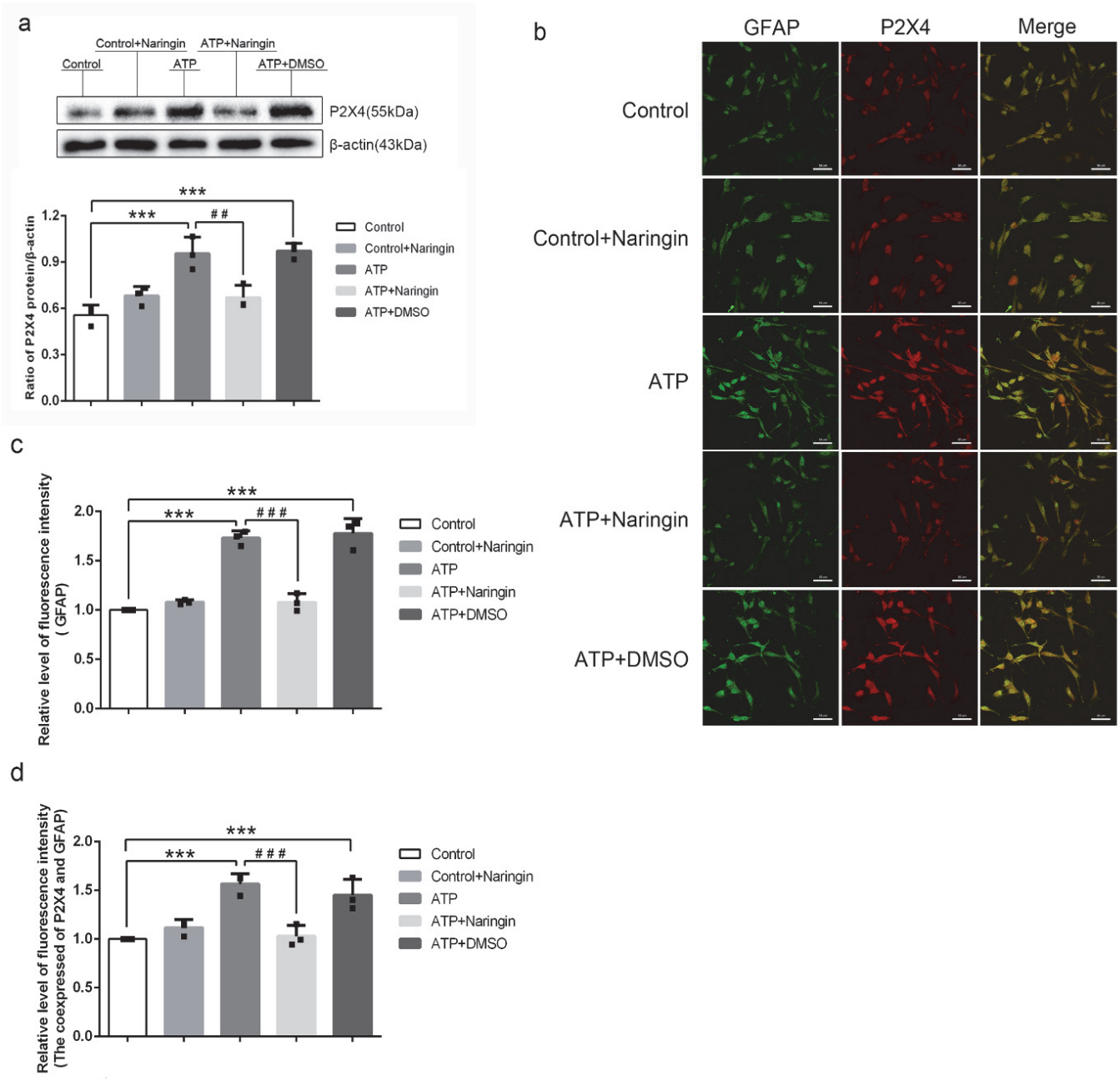

Fig. 1. Expression of P2X4R and coexpression of P2X4R and GFAP. (**a**) The expression of P2X4R in SGCs was measured using western blotting. The bar graph showed each group's mean relative densities of β-actin and P2X4R. (**b**) Coexpression of P2X4R and GFAP in SGCs; the green signal indicates GFAP staining with fluorescein isothiocyanate, and the red signal indicates P2X4R staining with tetramethyl rhodamine isothiocyanate, and the merge of coexpression of P2X4R and GFAP are shown in yellow. (**c**) Immunofluorescence analysis of GFAP expression on SGCs. (**d**) Immunofluorescence analysis of coexpression of P2X4R and GFAP. Compared with the control group, *** $P < 0.001$; compared with the ATP group, ## $P < 0.01$ and ### $P < 0.001$, $n = 3$. Scale bar = 50 μm.

Intracellular Ca^{2+} levels in SGCs

P2X4R is an ion channel type receptor whose activation leads to Ca^{2+} influx in SGCs. Intracellular Ca^{2+} in SGCs was measured using the BBcellProbe F03 method (Fig. 2). ATP activated P2X4R to increase intracellular Ca^{2+} concentrations ($P < 0.001$). Naringin had the opposite effect ($P < 0.01$).

Changes in the P38 MAPK/ERK signaling pathway

Intracellular Ca^{2+} modulates the P38 MAPK and ERK pathways and intracellular levels of P38 MAPK (Fig. 3a), P-p38 MAPK (Fig. 3b), ERK (Fig. 3c), and P-ERK (Fig. 3d) were measured using western blotting. ATP induced the upregulation of P-p38 MAPK ($P < 0.01$) and P-ERK ($P < 0.001$) levels, while naringin inhibited ATP-induced upregulation of P-p38 MAPK and P-ERK ($P < 0.01$) levels. These findings suggest that ATP can activate P38 MAPK and ERK signaling pathways, while naringin can inhibit the activation of these signaling pathways.

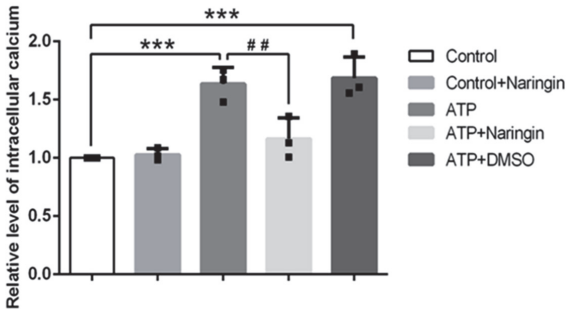

Fig. 2. Intracellular Ca^{2+} levels in SGCs in each group. The intracellular Ca^{2+} content in each group of SGCs was detected by BBcellProbe F03. Compared with the control group, *** $P < 0.001$; compared with the ATP group, ## $P < 0.01$, $n = 3$.

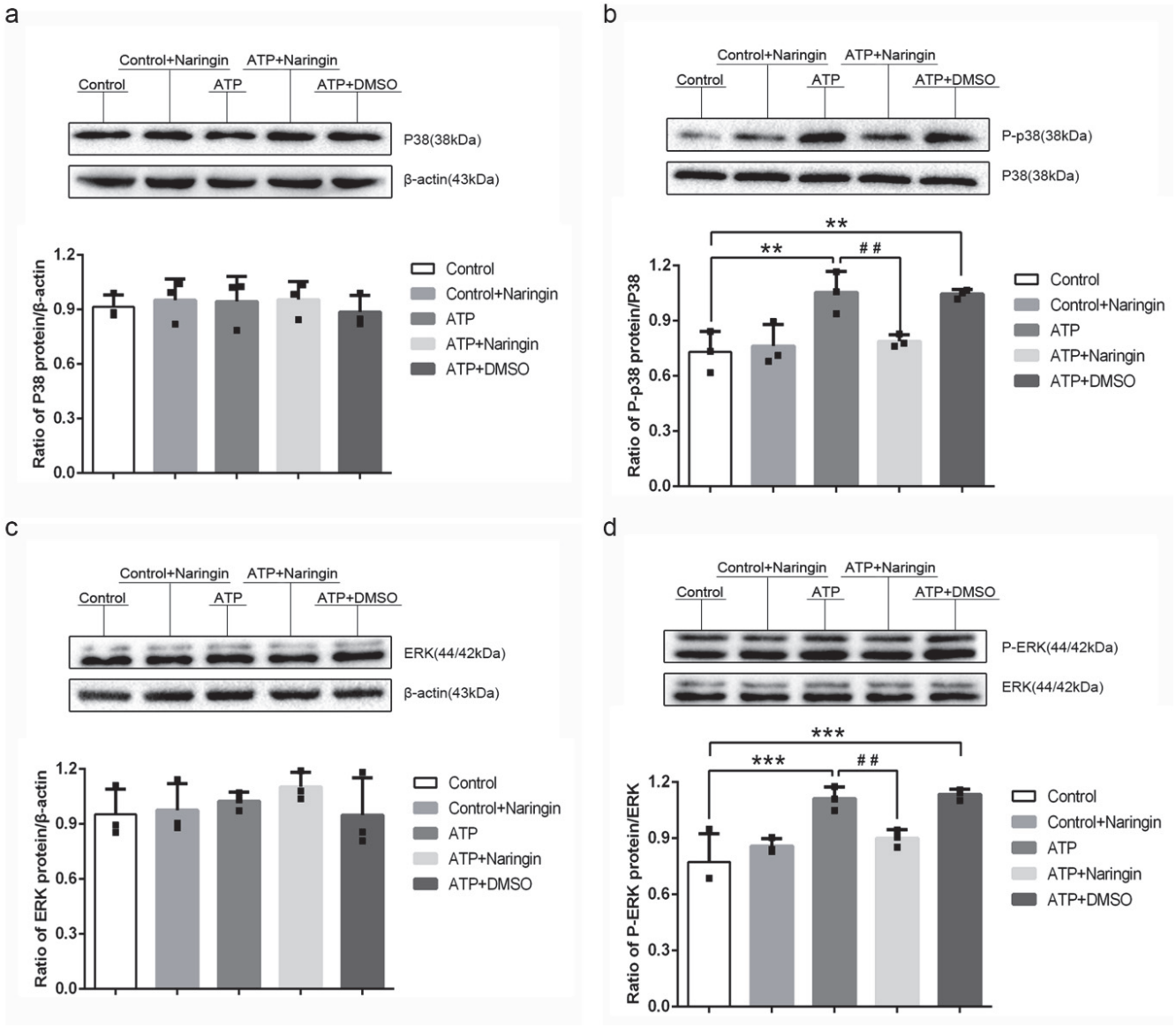

Fig. 3. Changes of the Ca^{2+}/P38 MAPK/ERK signaling pathway in SGCs. (**a, b**) Western blotting measures P38 and P-p38 levels in each group of SGCs. The bar graph shows each group's mean relative densities of P38/β-actin and P-p38/P38. (**c, d**) Western blotting measured the expression of ERK and P-ERK in each group of SGCs. The bar graph shows each group's mean relative densities of ERK/β-actin and P-ERK/ERK. Compared with the control group, ** $P < 0.01$ and *** $P < 0.001$; compared with the ATP group, ## $P < 0.01$, $n = 3$.

NF-κB activation in SGCs

NF-κB is a downstream signaling molecule of P38 MAPK, and activation of the P38 MAPK pathway activates the NF-κB signaling pathway, co-regulating physiological activities in cells. We used western blotting to measure P65 (Fig. 4a) and P-p65 (Fig. 4b) expression. P-p65 expression increased after ATP activation ($P < 0.05$), while naringin inhibited ATP-induced activation of NF-κB ($P < 0.05$).

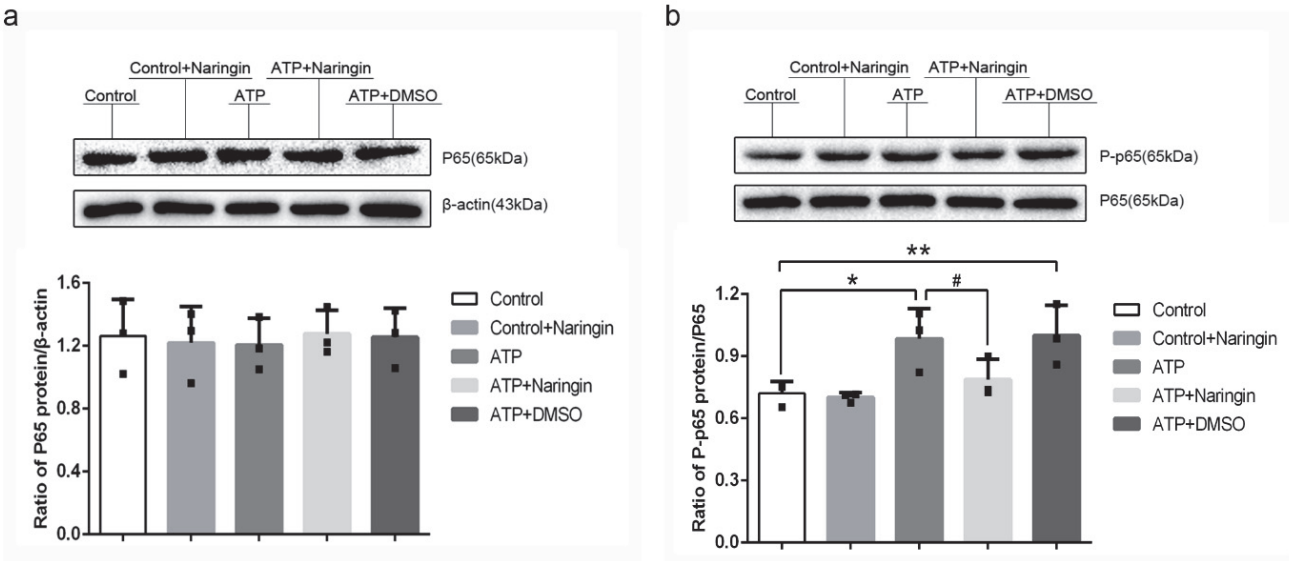

Fig. 4. P65 and P-p65 levels in each group of SGCs. (**a, b**) Western blotting to measure levels of P65 and P-p65 in SGCs. The bar graph shows each group's mean relative densities of P65/β-actin and P-p65/P65. Compared with the control group, * $P < 0.05$ and ** $P < 0.01$; compared with the ATP group, # $P < 0.05$, $n = 3$.

IL-1β and TNF-α levels

The NF-κB signaling pathway mediates the release of inflammatory factors, which is one of markers for SCGs activation. We used ELISA to detect the release of IL-1β (Fig. 5a) and TNF-α (Fig. 5b) from SGCs culture supernatants. The release of IL-1β ($P < 0.001$) and TNF-β ($P < 0.01$) from SGCs increased, and SGCs were activated under the stimulation of ATP, while naringin inhibited the release of IL-1β ($P < 0.001$) and TNF-α ($P < 0.01$).

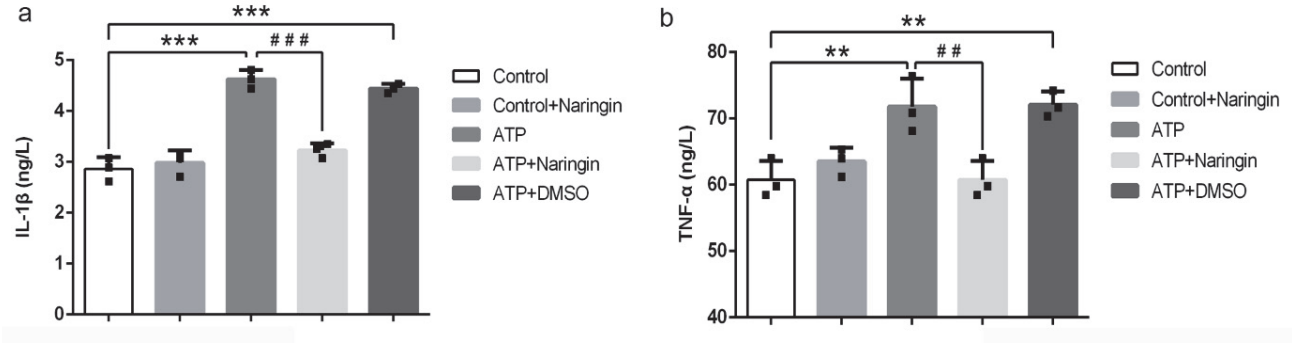

Fig. 5. Levels of IL-1β and TNF-α released by SGCs in each group. (**a, b**) ELISA detected the released levels of inflammatory factors IL-1β and TNF-α in SGCs. Compared with the control group, ** $P < 0.01$ and *** $P < 0.001$; compared with the ATP group, # # $P < 0.01$ and # # #$P < 0.001$, $n = 3$.

Discussion

SGCs are distributed around neurons in the peripheral nervous system, where they play supportive and protective roles (Milosavljević et al., 2020; Mohr et al., 2021). Glial cell activation has many manifestations, including upregulation of GFAP, release of inflammatory factors, *etc.* (Sung et al., 2019). The involvement of P2X4R in inflammation and pain has been extensively studied (Montilla et al., 2020; Zhang et al, 2020). Inhibition of P2X4R reduces TNF-α and IL-1β expression in microglia because of hypoxia and decreases microglial activation to reduce neuroinflammation (Li et al., 2011). ATP activates P2X4R, leading to the release of inflammatory factors (Stokes et al., 2017; Wang et al., 2020). In the present study, levels of GFAP, TNF-α and IL-1β in SGCs increased under ATP environment, and coexpression of P2X4R with GFAP increased after ATP stimulation, suggesting that SGCs are activated and P2X4R are upregulated under ATP environment.

Naringin is extracted from plants, and its anti-inflammatory effects have been extensively studied, for example, naringin reduces the expression of signaling molecules associated with inflammatory responses such as IL-1β, IL-8, TNF-α, and IL-6 (Chen et al., 2016, 2022). Our findings suggest that naringin reduces ATP-induced elevations of P2X4R expression in SGCs, leading to decreased release of inflammatory factors, reduced GFAP expression, and decreased SGC activation. As a second messenger, Ca^{2+} regulates many biological and pathological processes in cells and plays a vital role in activating various inflammation-related signaling pathways (Lu et al., 2017; Scheff and Gold, 2015; Scheff et al., 2013). Ca^{2+} regulates the P38 MAPK and ERK signaling pathways, and P38 MAPK and ERK signaling pathways play critical roles in cellular physiological activities such as inflammation, proliferation, and apoptosis (Akaishi et al., 2020; Zhou et al., 2019). P2X4R activation increases intracellular calcium content, activating the P38 MAPK pathway, confirming that P38 MAPK and Ca^{2+} are downstream signaling molecules of P2X4R (Ulmann et al., 2010). Naringin attenuates LPS-induced injury in human umbilical vein endothelial cells by inhibiting Ca^{2+} and reactive oxygen species accumulation in cells, reversing inflammation, and inhibiting cell death (Bi et al., 2016). In the present study, naringin significantly downregulated intracellular Ca^{2+} levels and decreased P-p38 and P-ERK levels, suggesting that naringin inhibits P2X4R activity, leading to a reduction in intracellular Ca^{2+} content and inhibiting P38 MAPK and ERK signaling pathway activation.

NF-κB plays a critical role in chronic pain and chronic inflammation, and P38 MAPK promotes the degradation of IκBα and activates NF-κB dimers to activatate the NF-κB signaling pathway, suggesting that P38 MAPK is an upstream signaling molecule of NF-κB (Lee et al., 2021; Shih et al., 2020). Naringin inhibits IκBα degradation and downregulates NF-κB activation to suppress the release of inflammatory factors, reducing the inflammatory effects of carrageenan in mice (Ahmad et al., 2015). In the present study, ATP activated the NF-κB signaling pathway and increased the release of TNF-α and IL-1β; naringin downregulated activation of the NF-κB signaling pathway. These findings suggest that naringin decreases the release of inflammatory factors via the Ca^{2+}-P38 MAPK/ERK-NF-κB signaling pathway to reduce SGC activation.

Conclusion

Naringin inhibits P2X4R expression in SGCs, and the Ca^{2+}-P38 MAPK/ERK-NF-κB signaling pathway may be involved in the pathophysiological process. The specific mechanism of action needs to be further investigated in future experiments, including explorations of the effect of naringin on the P2X4R function.

Acknowledgments
The authors would like to thank the Department of Physiology of Nanchang University for technical assistance.

Funding
This study was supported by Jiangxi Provincial Natural Science Foundation (grant Nos. 20232ACB206020 and 20202BAB206027), and the High-level and High-Skilled Leading Talent Training Project of Jiangxi Province in 2021 (grant No. 2022233 Jiangxi Province Human Resources and Social Security Department) also supported this work.

Conflict of interest
The authors have no conflict of interest to declare.

Ethical approval
The Ethical Committee of Nanchang University approved the study, and animals were treated according to the Guidelines for the Care and Use of Animals.

Consent for publication
The authors have provided their consent for the publication of this manuscript in its present form.

Data availability
The data supporting the findings are available from the corresponding author upon reasonable request.

Author contributions
Changshui Xu and Hongji Wang designed the study. Hongji Wang performed experiments and wrote the manuscript. Lisha Chen, Juping Xing, and Xiangchao Shi analyzed the data.

References

Ahmad SF, Attia SM, Bakheet SA, Zoheir KM, Ansari MA, Korashy HM, et al. (2015). Naringin attenuates the development of carrageenan-induced acute lung inflammation through inhibition of NF-kappaB, STAT3 and pro-inflammatory mediators and enhancement of IkappaBalpha and anti-inflammatory cytokines. Inflammation 38(2): 846–857. DOI: 10.1007/s10753-014-9994-y.

Akaishi T, Yamamoto S, Abe K (2020). The Synthetic Curcumin Derivative CNB-001 Attenuates Thrombin-Stimulated Microglial Inflammation by Inhibiting the ERK and p38 MAPK Pathways. Biol Pharm Bull 43(1): 138–144. DOI: 10.1248/bpb.b19-00699.

Bharti S, Rani N, Krishnamurthy B, Arya DS (2014). Preclinical evidence for the pharmacological actions of naringin: a review. Planta Med 80 (6): 437–451. DOI: 10.1055/s-0034-1368351.

Bi C, Jiang Y, Fu T, Hao Y, Zhu X, Lu Y (2016). Naringin inhibits lipopolysaccharide-induced damage in human umbilical vein endothelial cells via attenuation of inflammation, apoptosis and MAPK pathways. Cytotechnology 68(4): 1473–1487. DOI: 10.1007/s10616-015-9908-3.

Chen R, Gao S, Guan H, Zhang X, Gao Y, Su Y, et al. (2022). Naringin protects human nucleus pulposus cells against TNF-alpha-induced inflammation, oxidative stress, and loss of cellular homeostasis by enhancing autophagic flux via AMPK/SIRT1 activation. Oxid Med Cell Longev 2022: 7655142. DOI: 10.1155/2022/7655142.

Chen R, Qi QL, Wang MT, Li QY (2016). Therapeutic potential of naringin: an overview. Pharm Biol 54(12): 3203–3210. DOI: 10.1080/13880209.2016.1216131.

Chen Q, Wu H, Tao J, Liu C, Deng Z, Liu Y, et al. (2017). Effect of naringin on gp120-induced injury mediated by P2X7 receptors in rat primary cultured microglia. PloS One 12(8): e0183688. DOI: 10.1371/journal.pone.0183688.

Du E, Wang A, Fan R, Rong L, Yang R, Xing J, et al. (2022). Catestatin enhances ATP-induced activation of glial cells mediated by purinergic receptor P2X4. J Recept Signal Transduct Res 42(2): 160–168. DOI: 10.1080/10799893.2021.1878536.

Duveau A, Bertin E, Boué-Grabot E (2020). Implication of Neuronal Versus Microglial P2X4 Receptors in Central Nervous System Disorders. Neurosci Bull 36(11): 1327–1343. DOI: 10.1007/s12264-020-00570-y.

Eom S, Lee BB, Lee S, Park Y, Yeom HD, Kim TH, et al. (2021). Antioxidative and Analgesic Effects of Naringin through Selective Inhibition of Transient Receptor Potential Vanilloid Member 1. Antioxidants 11(1): 64. DOI: 10.3390/antiox11010064.

Hanani M (2022). How Is Peripheral Injury Signaled to Satellite Glial Cells in Sensory Ganglia? Cells 11(3): 512. DOI: 10.3390/cells11030512.

Hassan RA, Hozayen WG, Abo Sree HT, Al-Muzafar HM, Amin KA, Ahmed OM (2021). Naringin and Hesperidin Counteract Diclofenac-Induced Hepatotoxicity in Male Wistar Rats via Their Antioxidant, Anti-Inflammatory, and Antiapoptotic Activities. Oxid Med Cell Longev 2021: 9990091. DOI: 10.1155/2021/9990091.

He W, Wang Q, Sha W, Wang L, Li D, Chen G (2022). P2X4 Inhibition reduces microglia inflammation and apoptosis by NLRP3 and improves nervous system defects in rat brain trauma model. J Clin Neurosci 99: 224–232. DOI: 10.1016/j.jocn.2022.03.009.

Huang LY, Gu Y, Chen Y (2013). Communication between neuronal somata and satellite glial cells in sensory ganglia. Glia 61(10): 1571–1581. DOI: 10.1002/glia.22541.

Kohno K, Tsuda M (2021). Role of microglia and P2X4 receptors in chronic pain. Pain Rep 6(1): e864. DOI: 10.1097/PR9.0000000000000864.

Lee H, Jang JH, Kim SJ (2021). Malonic acid suppresses lipopolysaccharide-induced BV2 microglia cell activation by inhibiting the p38 MAPK/NF-kappaB pathway. Anim Cells Syst (Seoul) 25(2): 110–118. DOI: 10.1080/19768354.2021.1901781.

Lee JH, Kim W (2020). The Role of Satellite Glial Cells, Astrocytes, and Microglia in Oxaliplatin-Induced Neuropathic Pain. Biomedicines 8(9): 324. DOI: 10.3390/biomedicines8090324.

Li F, Guo N, Ma Y, Ning B, Wang Y, Kou L (2014). Inhibition of P2X4 suppresses joint inflammation and damage in collagen-induced arthritis. Inflammation 37(1): 146–153. DOI: 10.1007/s10753-013-9723-y.

Li F, Wang L, Li JW, Gong M, He L, Feng R, et al. (2011). Hypoxia induced amoeboid microglial cell activation in postnatal rat brain is mediated by ATP receptor P2X4. BMC Neurosci 12: 111. DOI: 10.1186/1471-2202-12-111.

Li L, Liu R, He J, Li J, Guo J, Chen Y, Ji K (2022). Naringin Regulates Microglia BV-2 Activation and Inflammation via the JAK/STAT3 Pathway. Evid Based Complement Alternat Med eCAM 2022: 3492058. DOI: 10.1155/2022/3492058.

Lu Y, Gu Y, Ding X, Wang J, Chen J, Miao C (2017). Intracellular Ca^{2+} homeostasis and JAK1/STAT3 pathway are involved in the protective effect of propofol on BV2 microglia against hypoxia-induced inflammation and apoptosis. PloS One 12(5): e0178098. DOI: 10.1371/journal.pone.0178098.

Milosavljević A, Jančić J, Mirčić A, Dožić A, Boljanović J, Milisavljević M, Ćetkovic M (2020). Morphological and functional characteristics of satellite glial cells in the peripheral nervous system. Folia Morphol (Warsz) 80(4): 745–755. DOI: 10.5603/FM.a2020.0141.

Mohr KM, Pallesen LT, Richner M, Vaegter CB (2021). Discrepancy in the Usage of GFAP as a Marker of Satellite Glial Cell Reactivity. Biomedicines 9(8): 1022. DOI: 10.3390/biomedicines9081022.

Montilla A, Mata GP, Matute C, Domercq M (2020). Contribution of P2X4 Receptors to CNS Function and Pathophysiology. Int J Mol Sci 21(15): 5562. DOI: 10.3390/ijms21155562.

Scheff NN, Gold MS (2015). Trafficking of Na+/Ca^{2+} exchanger to the site of persistent inflammation in nociceptive afferents. J Neurosci 35(22): 8423–8432. DOI: 10.1523/JNEUROSCI.3597-14.2015.

Scheff NN, Lu SG, Gold MS (2013). Contribution of endoplasmic reticulum Ca^{2+} regulatory mechanisms to the inflammation-induced increase in the evoked Ca^{2+} transient in rat cutaneous dorsal root ganglion neurons. Cell Calcium 54(1): 46–56. DOI: 10.1016/j.ceca.2013.04.002.

Shih JH, Tsai YF, Li IH, Chen MH, Huang YS (2020). Hp-s1 Ganglioside Suppresses Proinflammatory Responses by Inhibiting MyD88-Dependent NF-kappaB and JNK/p38 MAPK Pathways in Lipopolysaccharide-Stimulated Microglial Cells. Mar Drugs 18(10): 496. DOI: 10.3390/md18100496.

Stokes L, Layhadi JA, Bibic L, Dhuna K, Fountain SJ (2017). P2X4 Receptor Function in the Nervous System and Current Breakthroughs in Pharmacology. Front Pharmacol 8: 291. DOI: 10.3389/fphar.2017.00291.

Sung MS, Heo H, Eom GH, Kim SY, Piao H, Guo Y, Park SW (2019). HDAC2 Regulates Glial Cell Activation in Ischemic Mouse Retina. Int J Mol Sci 20(20): 51–59. DOI: 10.3390/ijms20205159.

Suurväli J, Boudinot P, Kanellopoulos J, Rüütel Boudinot S (2017). P2X4: A fast and sensitive purinergic receptor. Biomed J 40(5): 245–256. DOI: 10.1016/j.bj.2017.06.010.

Ulmann L, Hirbec H, Rassendren F (2010). P2X4 receptors mediate PGE2 release by tissue-resident macrophages and initiate inflammatory pain. EMBO J 29(14): 2290–2300. DOI: 10.1038/emboj.2010.126.

Wang H, Xu C (2022). A Novel Progress: Glial Cells and Inflammatory Pain. ACS Chem Neurosci 13(3): 288–295. DOI: 10.1021/acschemneuro.1c00607.

Wang M, Cai X, Wang Y, Li S, Wang N, Sun R, et al. (2020). Astragalin Alleviates Neuropathic Pain by Suppressing P2X4-Mediated Signaling in the Dorsal Root Ganglia of Rats. Front Neurosci 14: 570831. DOI: 10.3389/fnins.2020.570831.

Ying M, Liu H, Zhang T, Jiang C, Gong Y, Wu B, et al. (2017). Effect of artemisinin on neuropathic pain mediated by P2X(4) receptor in dorsal root ganglia. Neurochem Int 108: 27–33. DOI: 10.1016/j.neuint.2017.02.004.

Zhang WJ, Luo HL, Zhu ZM (2020). The role of P2X4 receptors in chronic pain: A potential pharmacological target. Biomed Pharmacother 129: 110447. DOI: 10.1016/j.biopha.2020.110447.

Zhou R, Yang X, Li X, Qu Y, Huang Q, Sun X, Mu D (2019). Recombinant CC16 inhibits NLRP3/caspase-1-induced pyroptosis through p38 MAPK and ERK signaling pathways in the brain of a neonatal rat model with sepsis. J Neuroinflammation 16: 239. DOI: 10.1186/s12974-019-1651-9.